Flow of a Third Grade Fluid between Coaxial Cylinders with Variable Viscosity

Muhammad Y. Malik, Azad Hussain, Sohail Nadeem, and Tasawar Hayat

Department of Mathematics, Quaid-i-Azam University 45320, Islamabad 44000, Pakistan

Reprint requests to M. Y. M.; E-mail: drmymalik@hotmail.com

Z. Naturforsch. **64a,** 588 – 596 (2009); received October 29, 2008 / revised March 26, 2009

The influence of temperature dependent viscosity on the flow of a third grade fluid between two coaxial cylinders is carried out. The heat transfer analysis is further analyzed. Homotopy analysis method is employed in finding the series solutions. The effects of pertinent parameters have been explored by plotting graphs.

Key words: Coaxial Cylinders; Variable Viscosity; Analytical Solutions.

1. Introduction

The subject of non-Newtonian fluid mechanics is very popular and an area of active research especially in industrial and technological problems. Examples of non-Newtonian fluids include tomatosauce, mustard, mayonnaise, toothpaste, asphalt, lava and ice, mud slides, snow avalanches, etc. The flow characteristics of non-Newtonian fluids are quite different from those of Newtonian fluids. The order of the governing equations for the non-Newtonian flow problem is in general higher than the corresponding Newtonian problem. Hence one needs the additional boundary/initial condition(s) for a unique solution. This issue of extra conditions has been discussed in detail by Rajagopal [1], Rajagopal and Gupta [2], Rajagopal et al. [3] and Rajagopal and Kaloni [4]. Furthermore the equations of non-Newtonian fluids are more nonlinear than the Newtonian fluids and to obtain an analytic solution is not an easy task. Despite all these challenges, various workers [5 – 15] are recently engaged in finding the analytical solutions for flows involving non-Newtonian fluids. Literature survey further indicates that very less attention has been given to the flows of non-Newtonian fluids with variable viscosity. The works of Massoudi and Christie [16], Pakdermirli and Yilbas [17] and Pantokratoras [18] may be mentioned in this direction.

The primary objective of this investigation is to model and analyze the flow between two coaxial cylinders. Constitutive equations of a third grade fluid are used. Two models of temperature dependent viscosity, namely Reynolds' and Vogel's, are considered. The flow is driven by the motion of an inner cylinder and a constant pressure gradient. The heat transfer analysis is also carried out. Analytical expressions of velocity and temperature are developed in each case by using a newly powerful technique namely the homotopy analysis method (HAM) [19 – 33]. Convergence of the series solution is carefully checked. Finally, the solutions are discussed with the help of graphs.

2. Problem Statement

Consider an incompressible and thermodynamic third grade fluid between two infinite coaxial cylinders. The flow is induced by a constant pressure gradient and motion of an inner cylinder. The outer cylinder is kept fixed. The heat transfer analysis is also taken into account. The dimensionless problems which can describe the flow and heat transfer are [16]

$$\begin{aligned}&\frac{\mathrm{d}\mu}{\mathrm{d}r}\frac{\mathrm{d}v}{\mathrm{d}r}+\frac{\mu}{r}\left(\frac{\mathrm{d}v}{\mathrm{d}r}+r\frac{\mathrm{d}^2v}{\mathrm{d}r^2}\right)\\&\quad+\frac{\Lambda}{r}\left(\frac{\mathrm{d}v}{\mathrm{d}r}\right)^2\left(\frac{\mathrm{d}v}{\mathrm{d}r}+3r\frac{\mathrm{d}^2v}{\mathrm{d}r^2}\right)=C,\end{aligned} \tag{1}$$

$$\frac{\mathrm{d}^2\theta}{\mathrm{d}r^2}+\frac{1}{r}\frac{\mathrm{d}\theta}{\mathrm{d}r}+\Gamma\left(\frac{\mathrm{d}v}{\mathrm{d}r}\right)^2\left[\mu+\Lambda\left(\frac{\mathrm{d}v}{\mathrm{d}r}\right)^2\right]=0, \tag{2}$$

$$v(r)=1,\quad \theta(r)=1;\quad r=1, \tag{3}$$

$$v(r)=0,\quad \theta(r)=0;\quad r=b, \tag{4}$$

with

$$r=\frac{\bar r}{R},\quad \Gamma=\frac{\mu_* V_0^2}{k(\theta_m-\theta_w)},\quad \theta=\frac{(\bar\theta-\theta_w)}{(\theta_m-\theta_w)},$$
$$\Lambda=\frac{2\beta_3 V_0^2}{R^2\mu_*},\quad C_1=\frac{\partial p}{\partial z},\quad C=\frac{C_1R^2}{\mu_* V_0}, \tag{5}$$
$$v=\frac{\bar v}{v_0},\quad \mu=\frac{\bar\mu}{\mu_*},$$

where μ_*, θ_m, V_0, Λ, β_3, and R as defined in [17] are the reference viscosity, a reference temperature (the bulk mean fluid temperature), and a reference velocity, respectively, Γ is related to the Prandtl number and Eckert number, β_3 is a dimensional third grade parameter, and Λ the dimensionless non-Newtonian viscosity.

3. Series Solutions for Reynolds' Model

Here the viscosity is expressed in the form

$$\mu=\mathrm{e}^{-M\theta} \tag{6}$$

which by Maclaurin's series can be written as

$$\mu=1-M\theta+O(\theta^2). \tag{7}$$

Note that $M=0$ corresponds to the case of constant viscosity. Invoking above equation into (1) and (2) one has

$$-M\frac{\mathrm{d}\theta}{\mathrm{d}r}\frac{\mathrm{d}v}{\mathrm{d}r}+\frac{1}{r}\frac{\mathrm{d}v}{\mathrm{d}r}-\frac{M}{r}\theta\frac{\mathrm{d}v}{\mathrm{d}r}+\frac{\mathrm{d}^2v}{\mathrm{d}r^2}-M\theta\frac{\mathrm{d}^2v}{\mathrm{d}r^2} + \frac{\Lambda}{r}\left(\frac{\mathrm{d}v}{\mathrm{d}r}\right)^3+3\Lambda\frac{\mathrm{d}^2v}{\mathrm{d}r^2}\left(\frac{\mathrm{d}v}{\mathrm{d}r}\right)^2=C, \tag{8}$$

$$\frac{\mathrm{d}^2\theta}{\mathrm{d}r^2}+\frac{1}{r}\frac{\mathrm{d}\theta}{\mathrm{d}r}+\Gamma\left(\frac{\mathrm{d}v}{\mathrm{d}r}\right)^2-\Gamma M\theta\left(\frac{\mathrm{d}v}{\mathrm{d}r}\right)^2 +\Lambda\Gamma\left(\frac{\mathrm{d}v}{\mathrm{d}r}\right)^4=0. \tag{9}$$

For HAM solution, we choose the following initial guesses:

$$v_0(r)=\frac{(r-b)}{(1-b)}, \tag{10}$$

$$\theta_0(r)=\frac{(r-b)}{(1-b)}. \tag{11}$$

The auxiliary linear operators are in the form

$$\mathcal{L}_{vr}(v)=v'', \tag{12}$$

$$\mathcal{L}_{\theta r}(\theta)=\theta'' \tag{13}$$

which satisfy

$$\mathcal{L}_{vr}(A_1+B_1r)=0, \tag{14}$$

$$\mathcal{L}_{\theta r}(A_2+B_2r)=0, \tag{15}$$

where A_1, A_2, B_1, B_2 are the constants.

If $p\in[0,1]$ is an embedding parameter and h_v and h_θ are auxiliary parameters then the problems at the zero- and mth-order are given by

$$(1-p)\mathcal{L}_v[\bar v(r,p)-v_0(r)]=p\hbar_v N_v[\bar v(r,p),\bar\theta(r,p)], \tag{16}$$

$$(1-p)\mathcal{L}_\theta[\bar\theta(r,p)-\theta_0(r)]=p\hbar_\theta N_\theta[\bar v(r,p),\bar\theta(r,p)], \tag{17}$$

$$\mathcal{L}_v[v_m(r)-\chi_m v_{m-1}(r)]=\hbar_v R_v(r), \tag{18}$$

$$\mathcal{L}_\theta[\theta_m(r)-\chi_m\theta_{m-1}(r)]=\hbar_\theta R_\theta(r), \tag{19}$$

$$\bar v(r,p)=\bar\theta(r,p)=1,\quad r=1, \tag{20}$$

$$\bar v(r,p)=\bar\theta(r,p)=0,\quad r=b. \tag{21}$$

The boundary conditions at the mth order are

$$\bar v_m(r,p)=\bar\theta_m(r,p)=0,\quad r=1, \tag{22}$$

$$\bar v_m(r,p)=\bar\theta_m(r,p)=0,\quad r=b. \tag{23}$$

In (16)–(19)

$$N_v[\bar v(r,p),\bar\theta(r,p)]= -M\frac{\mathrm{d}\theta}{\mathrm{d}r}\frac{\mathrm{d}v}{\mathrm{d}r}+\frac{1}{r}\frac{\mathrm{d}v}{\mathrm{d}r}-\frac{M}{r}\theta\frac{\mathrm{d}v}{\mathrm{d}r}+\frac{\mathrm{d}^2v}{\mathrm{d}r^2} -M\theta\frac{\mathrm{d}v2}{\mathrm{d}r^2}+\frac{\Lambda}{r}\left(\frac{\mathrm{d}v}{\mathrm{d}r}\right)^3+3\Lambda\frac{\mathrm{d}^2v}{\mathrm{d}r^2}\left(\frac{\mathrm{d}v}{\mathrm{d}r}\right)^2-C, \tag{24}$$

$$N_\theta[\bar v(r,p),\bar\theta(r,p)]=\frac{\mathrm{d}^2\theta}{\mathrm{d}r^2}+\frac{1}{r}\frac{\mathrm{d}\theta}{\mathrm{d}r}+\Gamma\left(\frac{\mathrm{d}v}{\mathrm{d}r}\right)^2 -\Gamma M\theta\left(\frac{\mathrm{d}v}{\mathrm{d}r}\right)^2+\Lambda\Gamma\left(\frac{\mathrm{d}v}{\mathrm{d}r}\right)^4, \tag{25}$$

$$R_v=-M\sum_{k=0}^{m-1}v'_{m-1-k}\theta'_k+\frac{1}{r}v'_{m-1}-\frac{M}{r}\sum_{k=0}^{m-1}v'_{m-1-k}\theta_k + v''_{m-1}-M\sum_{k=0}^{m-1}v''_{m-1}\theta_k+\frac{\Lambda}{r}\sum_{k=0}^{m-1}v'_{m-1-k}\sum_{l=0}^{k}v'_{k-l}v'_l + 3\Lambda\sum_{k=0}^{m-1}v'_{m-1-k}\sum_{l=0}^{k}v'_{k-l}v''_l-C(1-\chi_m), \tag{26}$$

$$R_\theta = \frac{1}{r}\theta'_{m-1} + \theta''_{m-1} + \Gamma \sum_{k=0}^{m-1} v'_{m-1-k} v'_k - \Gamma M \sum_{k=0}^{m-1} v'_{m-1-k} \sum_{l=0}^{k} v'_{k-l}\theta_l + \Lambda\Gamma \sum_{k=0}^{m-1}\left(\sum_{l=0}^{m-1-k} v'_{m-1-k-l}v'_l\right)\left(\sum_{s=0}^{k} v'_{k-s}v'_s\right). \tag{27}$$

By Mathematica the solutions of (26) and (27) can be written as

$$v_m(r) = \sum_{n=0}^{3m} a_{m,n} r^n, \quad m \geq 0, \qquad \theta_m(r) = \sum_{n=0}^{3m+1} d_{m,n} r^n, \quad m \geq 0, \tag{28}$$

where $a_{m,n}$ and $d_{m,n}$ are constants which can be determined on substituting (28) into (18) and (19).

4. Series Solutions for Vogel's Model

Here

$$\mu = \mu_* \exp\left[\frac{A}{(B+\theta)} - \theta_w\right] \tag{29}$$

which by Maclaurins' series reduces to

$$\mu = \frac{C}{C^*}\left(1 - \frac{\theta A}{B^2}\right). \tag{30}$$

Invoking above expression, (1) and (2) become

$$\frac{-AC}{C^*B^2}\frac{\mathrm{d}\theta}{\mathrm{d}r}\frac{\mathrm{d}v}{\mathrm{d}r} + \frac{C}{rC^*}\frac{\mathrm{d}v}{\mathrm{d}r} - \frac{AC}{rC^*B^2}\theta\frac{\mathrm{d}v}{\mathrm{d}r} + \frac{AC}{C^*B^2}\theta\frac{\mathrm{d}^2v}{\mathrm{d}r^2} + \frac{\Lambda}{r}\left(\frac{\mathrm{d}v}{\mathrm{d}r}\right)^3 + 3\Lambda\left(\frac{\mathrm{d}v}{\mathrm{d}r}\right)^2 = C, \tag{31}$$

$$\frac{d^2\theta}{\mathrm{d}r^2} + \frac{1}{r}\frac{\mathrm{d}\theta}{\mathrm{d}r} + \frac{\Gamma C}{C^*}\left(\frac{\mathrm{d}v}{\mathrm{d}r}\right)^2 - \frac{AC}{C^*B^2}\theta\left(\frac{\mathrm{d}v}{\mathrm{d}r}\right)^2 + \Lambda\Gamma\left(\frac{\mathrm{d}v}{\mathrm{d}r}\right)^4 = 0. \tag{32}$$

With the following initial guesses and auxiliary linear operators

$$v_{0v}(r) = \frac{(r-b)}{(1-b)}, \tag{33}$$

$$\theta_{0v}(r) = \frac{(r-b)}{(1-b)}, \tag{34}$$

$$\mathcal{L}_{vv}(v) = v'', \tag{35}$$

$$\mathcal{L}_{\theta v}(\theta) = \theta'' \tag{36}$$

the mth-order deformation problems are

$$\mathcal{L}_{vr}[v_m(r) - \chi_m v_{m-1}(r)] = \hbar_v R_{vr}(r), \tag{37}$$

$$\mathcal{L}_{\theta r}[\theta_m(r) - \chi_m \theta_{m-1}(r)] = \hbar_\theta R_{\theta r}(r), \tag{38}$$

$$R_{vv} = -\frac{AC}{C^*B^2}\sum_{k=0}^{m-1} v'_{m-k-1}\theta'_k + \frac{C}{rC^*}v'_{m-1} - \frac{AC}{rC^*B^2}\sum_{k=0}^{m-1} v'_{m-k-1}\theta_k + \frac{C}{C^*}v''_{m-1} - \frac{AC}{C^*B^2}\sum_{k=0}^{m-1} v''_{m-k-1}\theta_k + \frac{\Lambda}{r}\sum_{k=0}^{m-1} v'_{m-k-1}\sum_{l=0}^{k} v'_{k-l}v'_l + 3\Lambda\sum_{k=0}^{m-1} v'_{m-k-1}\sum_{l=0}^{k} v'_{k-l}v''_l - C(1-\chi_m), \tag{39}$$

$$R_{\theta v} = \frac{1}{r}\theta'_{m-1} + \theta''_{m-1} + \frac{C}{C^*}\Gamma\sum_{k=0}^{m-1} v'_{m-k-1}v'_k - \Gamma\frac{AC}{C^*B^2}\sum_{k=0}^{m-1} v'_{m-k-1}\sum_{l=0}^{k} v'_{k-l}\theta_l + \Lambda\Gamma\sum_{k=0}^{m-1}\left(\sum_{l=0}^{m-1-k} v'_{m-1-k-l}v'_l\right)\left(\sum_{s=0}^{k} v'_{k-s}v'_s\right). \tag{40}$$

The expressions of v_m and θ_m are finally given by

$$v_m(r) = \sum_{n=0}^{3m} a'_{m,n} r^n, \quad m \geq 0, \tag{41}$$

$$\theta_m(r) = \sum_{n=0}^{3m+1} d'_{m,n} r^n, \quad m \geq 0. \tag{42}$$

5. Graphical Results and Discussion

In order to report the convergence of the obtained series solutions and the effects of sundry parameters in the present investigation we plotted Figures 1 – 26. Particularly the variations of C, Γ, Λ, M, A, and B are seen. Here C is relevant to the pressure drop, Γ to the viscous dissipation, Λ the non-Newtonian behaviour of the fluid, A and B the variations of viscosity of Vogel's model and M the variations of viscosity of Reynolds' model. The Figures 1 – 8 have been sketched for the Reynolds' model while Figures 9 – 26 correspond to

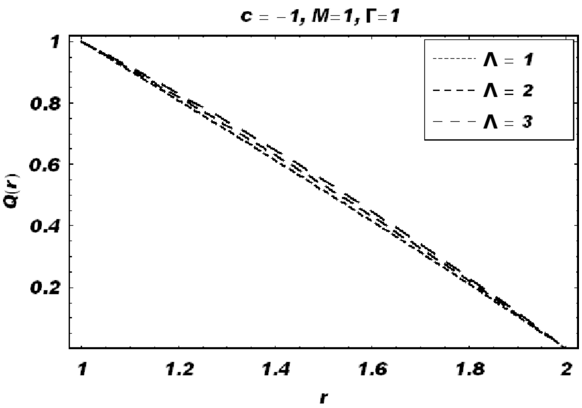

Fig. 1. Temperature profile along the radial distance for different values of Λ for the Reynolds' model.

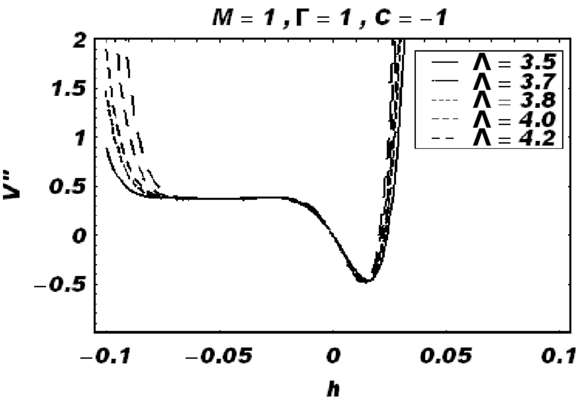

Fig. 2. h-curve for different values of variable viscosity parameter Λ for the Reynolds' model.

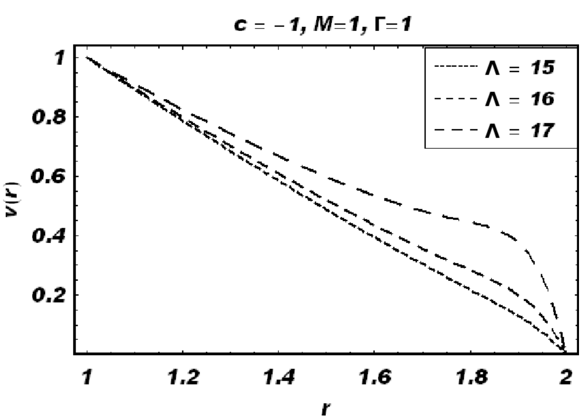

Fig. 3. Velocity profile along the radial distance for different values of Λ for the Reynolds' model.

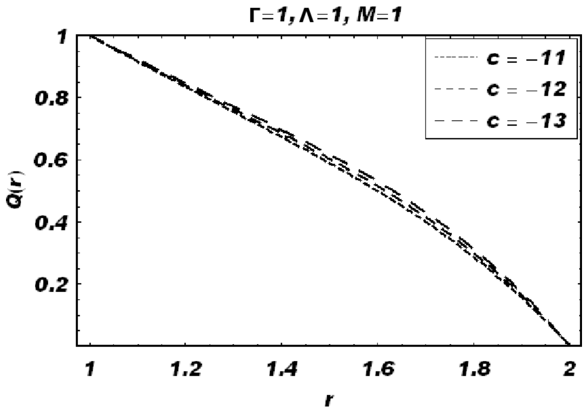

Fig. 4. Temperature profile along the radial distance for different values of C for the Reynolds' model.

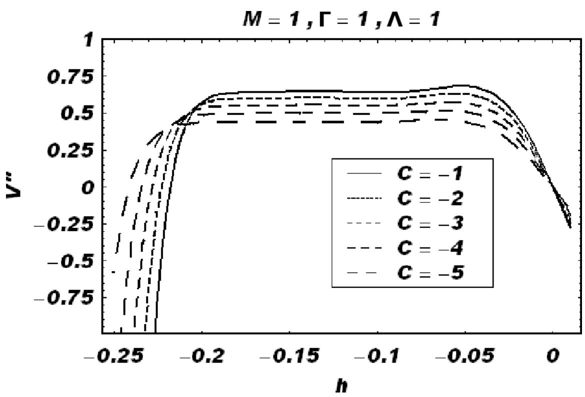

Fig. 5. h-curve for different values of variable viscosity parameter C for the Reynolds' model.

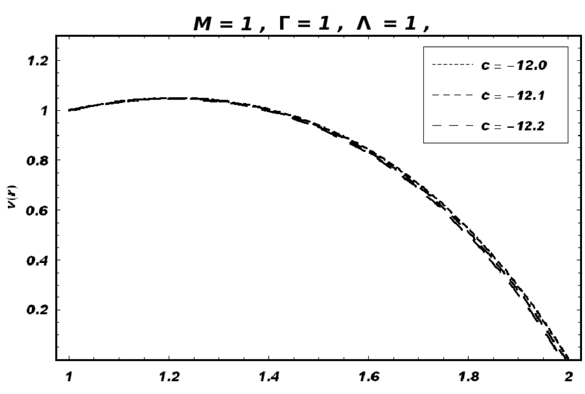

Fig. 6. Velocity profile along the radial distance for different values of C for the Reynolds' model.

the case of Vogel's model. Figures 1 and 3 show the temperature and velocity profiles along the radial distance for different values of Λ. It is found that velocity and temperature fields increase by increasing Λ. Figure 2 is prepared to see the convergence region for different values of Λ. The effects of constant pressure

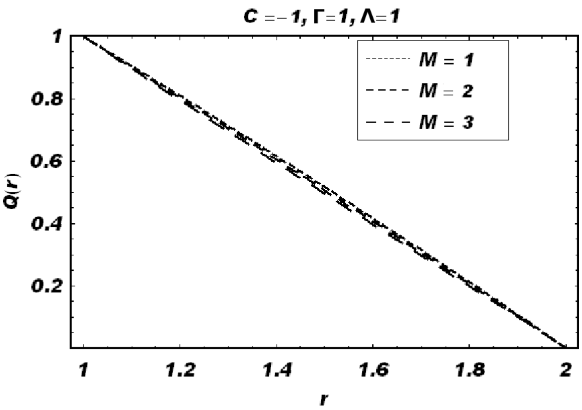

Fig. 7. Temperature profile along the radial distance for different values of M for the Reynolds' model.

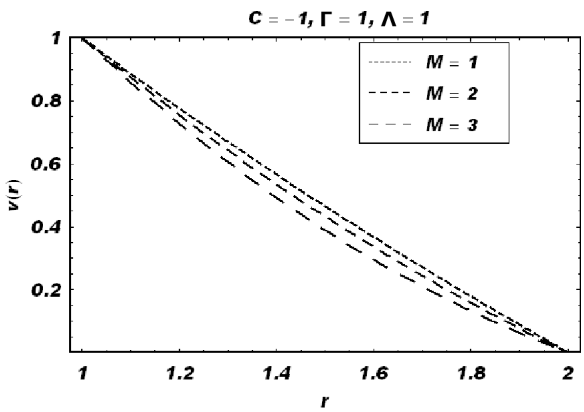

Fig. 8. Velocity profile along the radial distance for different values of M for the Reynolds' model.

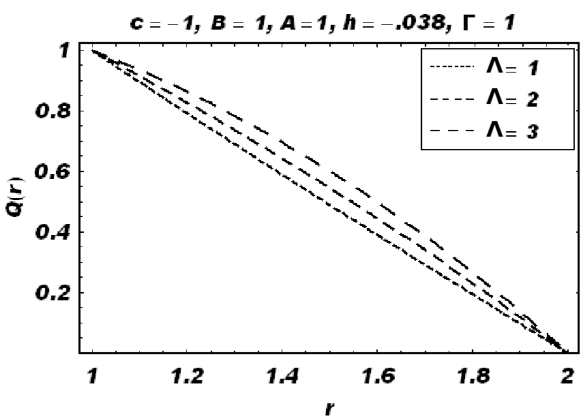

Fig. 9. Temperature profile along the radial distance for different values of Λ for Vogel's model.

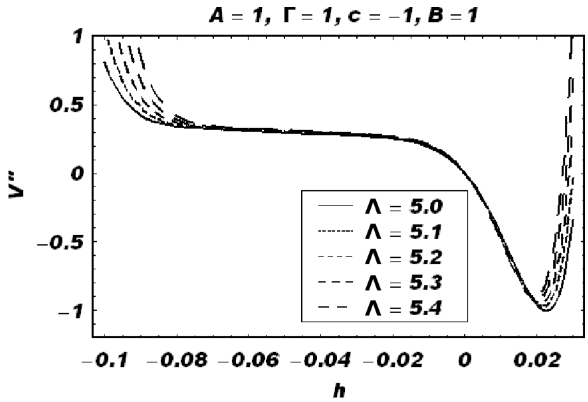

Fig. 10. h-curve for different values of Λ for Vogel's model.

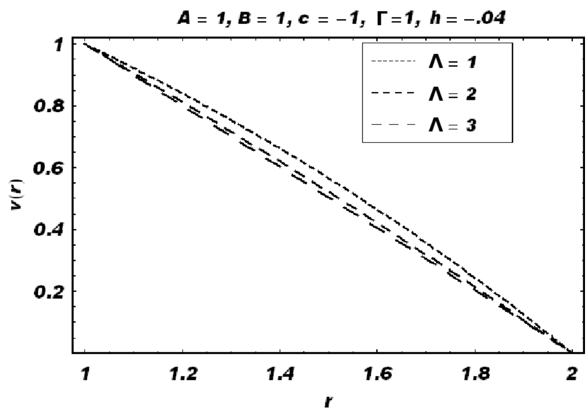

Fig. 11. Velocity profile along the radial distance for different values of Λ for Vogel's model.

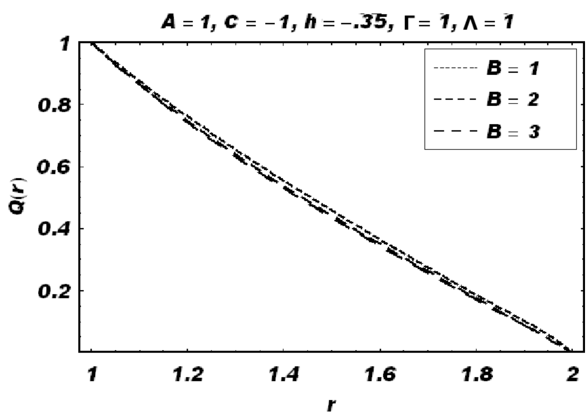

Fig. 12. Temperature profile along the radial distance for different values of B for Vogel's model.

gradient on the temperature and velocity can be seen in Figures 4 and 6. It is observed from these figures that with an increase in C, both the velocity and temperature decrease. Figure 7 is prepared for the temperature distribution when different values of M are used.

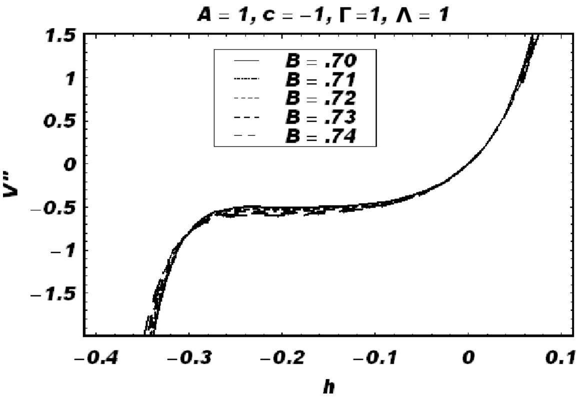

Fig. 13. h-curve for different values of B for Vogel's model.

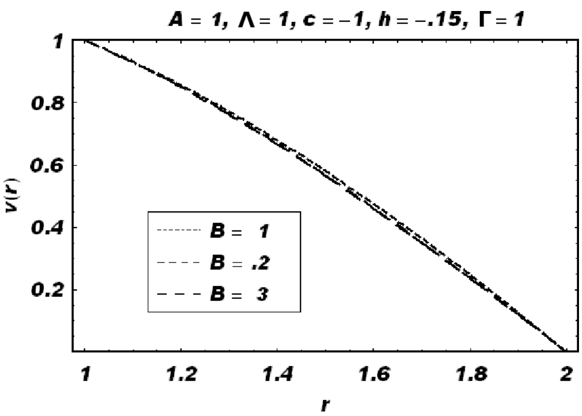

Fig. 14. Velocity profile along the radial distance for different values of B for Vogel's model.

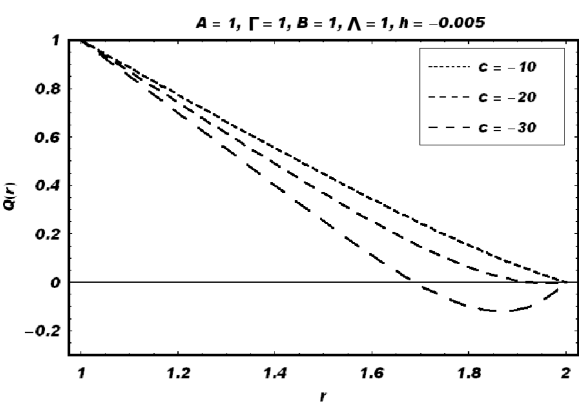

Fig. 15. Temperature profile along the radial distance for different values of C for Vogel's model.

It shows that with an increase in M the temperature decreases. This happens because with increasing M the viscosity decreases and decrease of viscosity effects the viscous dissipation which causes the decrease in

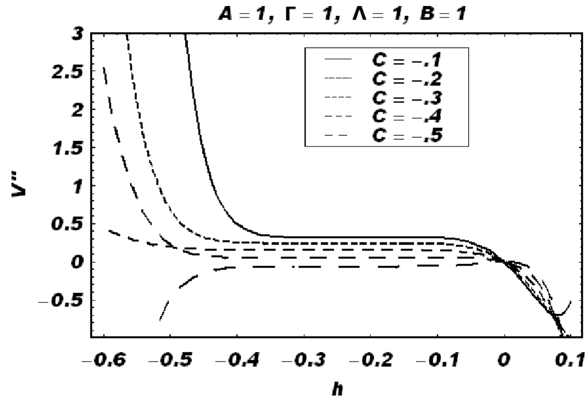

Fig. 16. h-curve for different values of variable viscosity parameter C for Vogel's model.

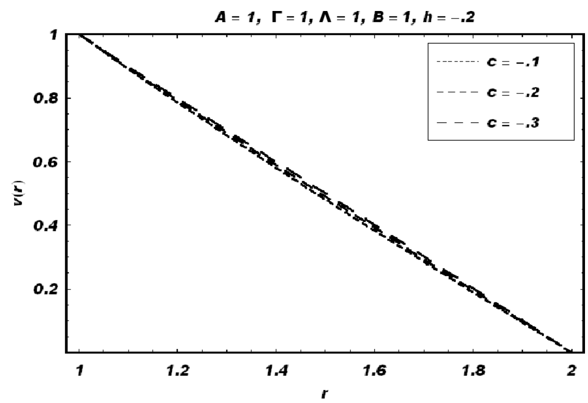

Fig. 17. Velocity profile along the radial distance for the different values of C for Vogel's model.

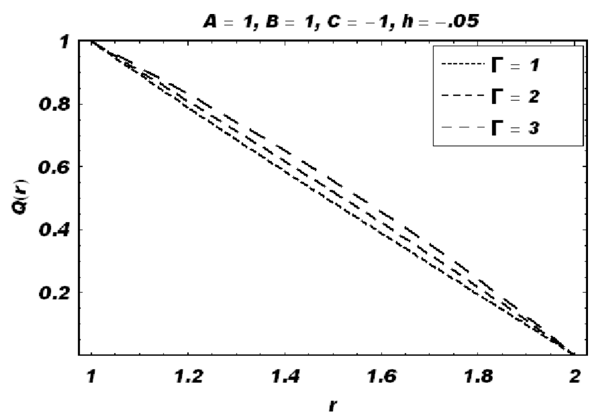

Fig. 18. Temperature profile along the radial distance for different values of Γ for Vogel's model.

temperature. Figure 8 is plotted for the velocity distribution against r when different values of M are taken into account. It is seen from the figure that by increas-

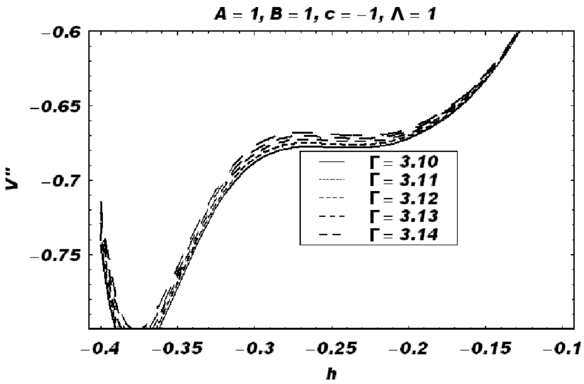

Fig. 19. h-curve for different values of Γ for Vogel's model.

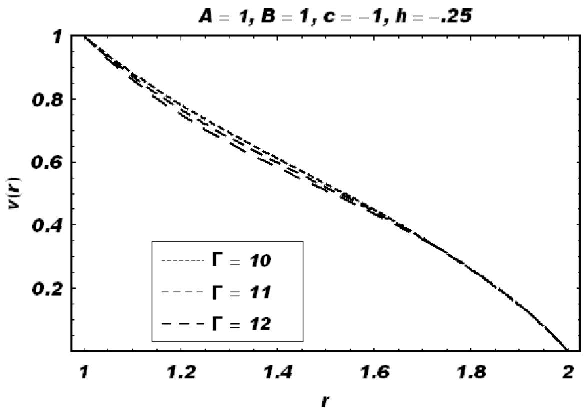

Fig. 20. Velocity profile along the radial distance for different values of Γ for Vogel's model.

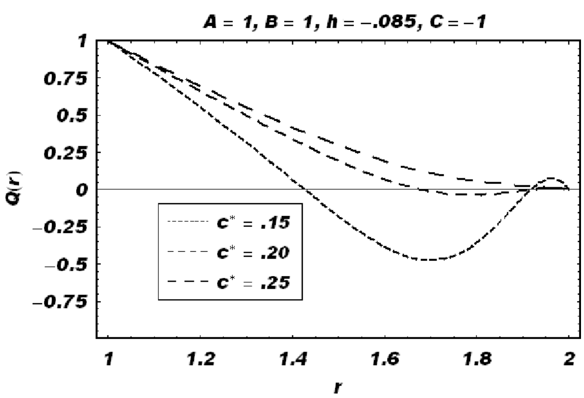

Fig. 21. Temperature profile along the radial distance for different values of C^* for Vogel's model.

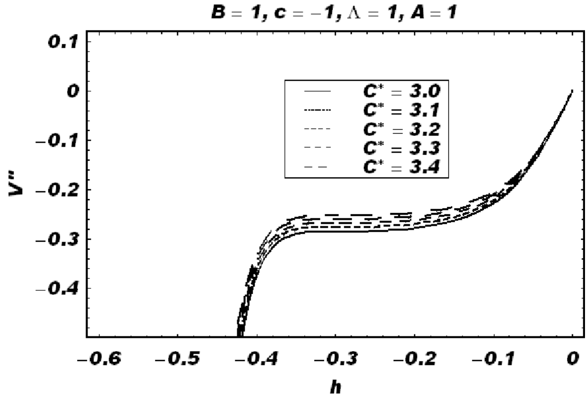

Fig. 22. h-curve for different values of C^* for Vogel's model.

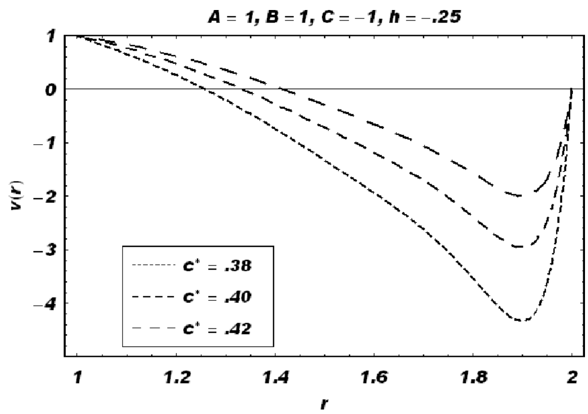

Fig. 23. Velocity profile along the radial distance for different values of C^* for Vogel's model.

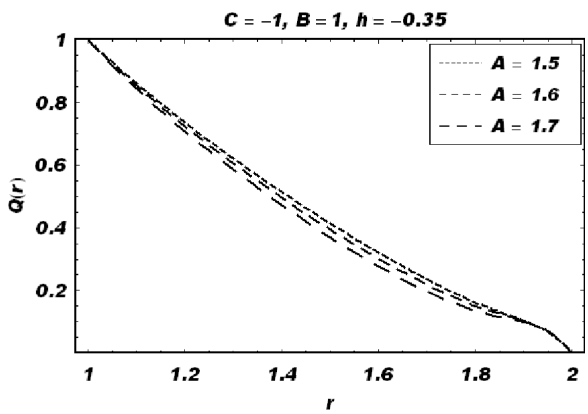

Fig. 24. Temperature profile along the radial distance for different values of A for Vogel's model.

ing M, the velocity decreases. Figures 9 and 11 illustrate the temperature and velocity profiles along the radial distance for different values of Λ. It is found that both velocity and temperature increase when Λ increases. Figure 10 is prepared to see the convergence region for different values of Λ. Figures 12 and 14 show the temperature and velocity profiles along the

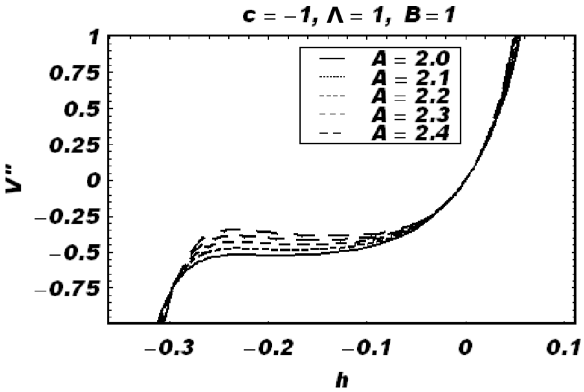

Fig. 25. h-curve for different values of variable viscosity parameter A for Vogel's model.

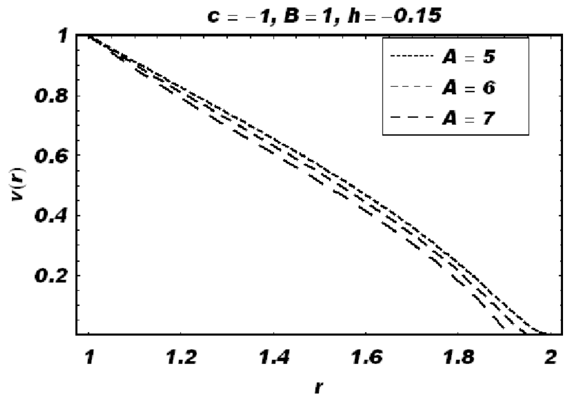

Fig. 26. Velocity profile along the radial distance for different values of A for Vogel's model.

radial distance for different values of B. It is found that the behaviour of B on the velocity and temperature is similar to Λ. Figure 13 is prepared to see the convergence region for different values of B. The effects of constant pressure gradient on the temperature and velocity are displayed in Figures 15 and 17. These figures indicate that by increasing C, both the velocity and temperature increase. Figure 16 is prepared to see the convergence region for different values of C. The effects of Brikmann number Γ are shown in Figures 18 and 20. It is found that with an increase in Γ, velocity decreases and temperature increases. As pointed out in [16], the concept of the viscous dissipation is of great value for many non-Newtonian fluids, such as polymer processing, which is at very high temperatures, and flows encountered in glacier physics. Figure 19 is prepared to see the convergence region for different values of Γ. Figures 21 and 23 show the temperature and velocity profiles along the radial distance for different values of C^*. Both velocity and temperature increase when C^* is increased. Figure 22 is prepared to see the convergence region for different values of C^*. Figures 24 and 26 show the temperature and velocity profiles along the radial distance for different values of A. Figure 25 is prepared to see the convergence region for different values of A. It is noticed from Figures 24 and 26 that both temperature and velocity decrease when A increases.

Acknowledgement

The authors are grateful for the anonymous referee for the valuable suggestions.

[1] K. R. Rajagopal, Acta Cienca India **18**, 1 (1982).
[2] K. R. Rajagopal and A. S. Gupta, Meccanica **19**, 158 (1984).
[3] K. R. Rajagopal, A. Z. Szeri, and W. Troy, Int. J. Nonlinear Mech. **21**, 279 (1986).
[4] K. R. Rajagopal and P. N. Kaloni, Some remarks on boundary conditions for fluids of differential type, in G. A. C. Graham, S. K. Malik (Eds), Continium Mechanics and its Applications, Hemisphere, New York (1989) pp. 935 – 942.
[5] C. Fetecau, T. Hayat, Co. Fetecau, and N. Ali, Nonlinear Analysis: Real World Applications **9**, 1236 (2008).
[6] D. Vieru, M. Nazar, Co. Fetecau, and C. Fetecau, Computers & Mathematics with Applications **55**, 1644 (2008).
[7] D. Vieru, T. Hayat, Co. Fetecau, and C. Fetecau, Appl. Math. Comp. **197**, 76 (2008).
[8] W. C. Tan and T. Masuoka, Phys. Fluids **17**, 023101 (2005).
[9] C. I. Chen, C. K. Chen, and Y. T. Yang, Heat Mass Transf. **40**, 203 (2004).
[10] P. D. Ariel, T. Hayat, and S. Asghar, Acta Mech. **187**, 29 (2006).
[11] P. D. Ariel, Int. J. Eng. Sci. **41**, 1267 (2003).
[12] S. Nadeem, S. Asghar, T. Hayat, and M. Hussain, Meccanica **43**, 496 (2008).
[13] T. Hayat and N. Ali, Appl. Math. Modelling **32**, 761 (2008).
[14] T. Hayat, S. Nadeem, A. M. Siddiqui, and S. Asghar, Appl. Math. Lett. **17**, 609 (2004).
[15] T. Hayat, R. Naz, and S. Asghar, Appl. Math. Comput. **157**, 103 (2004).
[16] M. Massoudi and I. Christie, Int. J. Nonlinear Mech. **30**, 687 (1995).

[17] M. Pakdermirli and B. S. Yilbas, Int. J. Nonlinear Mech. **41**, 432 (2006).
[18] A. Pantokratoras, Int. J. Thermal. Sci. **45**, 378 (2006).
[19] S. J. Liao, Introduction to homotopy analysis method. Boca Raton: Chapman & Hall/CRC Press, 2003.
[20] S. J. Liao, Appl. Math. Comput. **147**, 499 (2004).
[21] S. J. Liao, J. Fluid Mech. **385**, 101 (1999).
[22] S. J. Liao, Comm. Nonlinear Sci. Numer. Simul. **11**, 326 (2006).
[23] S. Abbasbandy, Phys. Lett. A **360**, 109 (2006).
[24] S. Abbasbandy, Int. Comm. Heat Mass Transf. **34**, 380 (2007).
[25] Z. Abbas and T. Hayat, Int. J. Heat and Mass Transfer **51**, 1024 (2008).
[26] T. Hayat, Z. Abbas, and M. Sajid, Phys. Lett. A **358**, 396 (2006).
[27] M. Sajid, T. Hayat, and S. Asghar, Phys. Lett. A **355**, 18 (2006).
[28] T. Hayat, Z. Abbas, and M. Sajid, Phys. Lett. A **372**, 2400 (2008).
[29] M. Sajid and T. Hayat, Trans. Porous Media **71**, 173 (2008).
[30] T. Hayat and Z. Abbas, Z. Angew. Math. Phys. **59**, 124 (2008).
[31] S. J. Liao, Comm. Nonlinear Sci. Numer. Simul. **14**, 983 (2009).
[32] S. Abbasbandy, Y. Tan, and S. J. Liao, Appl. Math. Comput. **188**, 1794 (2007).
[33] F. Talay Akyildiz, K. Vajravelu, and S.-J. Liao, Chaos, Solitons and Fractals **39**, 1073 (2009).